PHYSICAL REVIEW B **93**, 161403(R) (2016)

Orbital-symmetry-selective spin characterization of Dirac-cone-like state on W(110)

K. Miyamoto,[1,2,*] H. Wortelen,[1] H. Mirhosseini,[3] T. Okuda,[2] A. Kimura,[4] H. Iwasawa,[2] K. Shimada,[2] J. Henk,[5] and M. Donath[1]

[1]*Physikalisches Institut, Westfälische Wilhelms-Universität Münster, Wilhelm-Klemm-Straße 10, 48149 Münster, Germany*

[2]*Hiroshima Synchrotron Radiation Center, Hiroshima University, 2-313 Kagamiyama, Higashi-Hiroshima 739-0046, Japan*

[3]*Max-Planck-Institut für Mikrostrukturphysik, Weinberg 2, 06120 Halle, Germany*

[4]*Graduate School of Science, Hiroshima University, 1-3-1 Kagamiyama, Higashi-Hiroshima 739-8526, Japan*

[5]*Institut für Physik, Martin-Luther-Universität Halle-Wittenberg, Von-Seckendorff-Platz 1, 06120 Halle, Germany*

(Received 20 January 2016; revised manuscript received 4 March 2016; published 8 April 2016)

The surface of W(110) exhibits a spin-orbit-induced Dirac-cone-like surface state, which is of mainly d_{z^2} orbital character near $\overline{\Gamma}$, although it is strongly influenced by the twofold C_{2v} surface symmetry. Its distinctive **k**-dependent spin polarization along $\overline{\Gamma}\,\overline{H}$ is revealed by spin- and angle-resolved photoemission excited with *p*- and *s*-polarized light. The spin texture of the surface state is found to change sign upon switching from *p*- to *s*-polarized light. Based on electronic-structure calculations, this behavior is explained by the orbital composition of the Dirac-cone-like state. The dominant part of the state has even mirror symmetry and is excited by *p*-polarized light. A minor part with odd symmetry is excited by *s*-polarized light and exhibits a reversed spin polarization. Our study demonstrates in which way spin-orbit interaction combines the spin degree of freedom with the orbital degree of freedom and opens a way to manipulate the spin information gathered from the Dirac-cone-like surface state by light. Our results prove that "spin control" is not restricted to topological surface states with *p*-type orbital symmetry in topological insulators.

DOI: 10.1103/PhysRevB.93.161403

Topological insulators (TI) have attracted great attention as key materials to generate and manipulate spin currents without magnetic fields [1–3]. The lack of space-inversion symmetry at the surface of a TI leads to Dirac-cone-like, so-called topological surface states (TSS) with helical spin texture induced by strong spin-orbit interaction [4].

The interplay between spin-orbit interaction, orbital symmetries, and spin polarization has become a research focus in studies on the TSS of the prototypical TI Bi_2Se_3. Recently, a fascinating idea was presented: the manipulation and control of the spin polarization of the photoemission signal from the Dirac-cone-like TSS by a proper choice of the light polarization, experimental geometry, and photon energy [5–11]. This effect is currently highly debated in view of optospintronics applications. However, detailed studies of the photoelectron spin features are so far restricted to almost isotropic and ideal Dirac-cone-like TSS of *p*-type orbital symmetry in materials with C_{3v} surface symmetry. Hence, the fundamental relation between intrinsic spin polarization and measured spin signal has become a focus of interest recently [12–16].

For a surface state on W(110) within a spin-orbit-induced symmetry gap [17,18], we recently found a Dirac-cone-like dispersion behavior with a spin texture reminiscent of a TSS [19]. In contrast to a TSS, it is derived from *d* orbitals and the surface has twofold symmetry (C_{2v}). The latter is responsible for a flattened dispersion behavior along $\overline{\Gamma}\,\overline{N}$ compared with a linear dispersion along $\overline{\Gamma}\,\overline{H}$ [20] and along $\overline{\Gamma}\,\overline{S}$ [19,21]. Note that only $\overline{\Gamma}\,\overline{N}$ and $\overline{\Gamma}\,\overline{H}$ lie in mirror planes. Based on several experimental and theoretical studies, the state, around $\overline{\Gamma}$, has predominantly d_{z^2} orbital symmetry, belonging to the Σ_1 (single-group) representation, with significant Σ_3 and minor Σ_2 and Σ_4 contributions [20,22–25]. For the $\overline{\Gamma}\,\overline{H}$ mirror-plane direction, photoemission calculations expect high intensity for excitation with *p*-polarized light, based on its dominant even symmetry with respect to the mirror plane, and only small intensity for *s*-polarized light [22]. Interestingly and again reminiscent of the TSS behavior, the calculations predict a spin reversal on changing the light polarization from *p* to *s*.

In this Rapid Communication, we put the predicted spin texture of the W(110) surface state in the mirror-plane direction $\overline{\Gamma}\,\overline{H}$ to the experimental test. We use angle-resolved photoelectron spectroscopy (ARPES) with spin analysis for the photoelectrons to reveal the orbital-symmetry-selective spin texture of the surface state. We chose a highly symmetric experimental geometry: The electrons are excited by linear polarized synchrotron light and the momenta of the electrons are varied in a mirror plane of the crystal.

A clean surface of W(110) was obtained and evaluated by the same procedures as described earlier [19,20]. The experiments have been performed at two beamlines at the Hiroshima Synchrotron Radiation Center (HiSOR): spin-integrated ARPES with light from a linear undulator at beamline BL-1 and spin-resolved ARPES with light from a quasi-periodic variably polarizing undulator [26] at beamline BL-9B, equipped with highly efficient three-dimensional spin-polarization analysis of the ESPRESSO machine [27,28].

At BL-9B, the electric field vector of the synchrotron light can be switched between parallel (*p* polarization) and perpendicular (*s* polarization) to the plane spanned by the surface normal and the photoelectron propagation vectors by changing the magnetic phase of the undulator. In order to reduce higher harmonics contributions, a quasiperiodic magnet array is used. As a consequence, the generated *p*-polarized light is almost fully polarized (>99.95%), while the *s* polarization amounts to only about 90% with a 10% contribution of *p* polarization at a photon energy of $h\nu = 43$ eV, caused by the quasiperiodicity of the magnet. This admixture of *p*-polarized light in the nominal *s*-polarized light becomes a critical issue

*kmiyamoto@hiroshima-u.ac.jp

 ©2016 American Physical Society

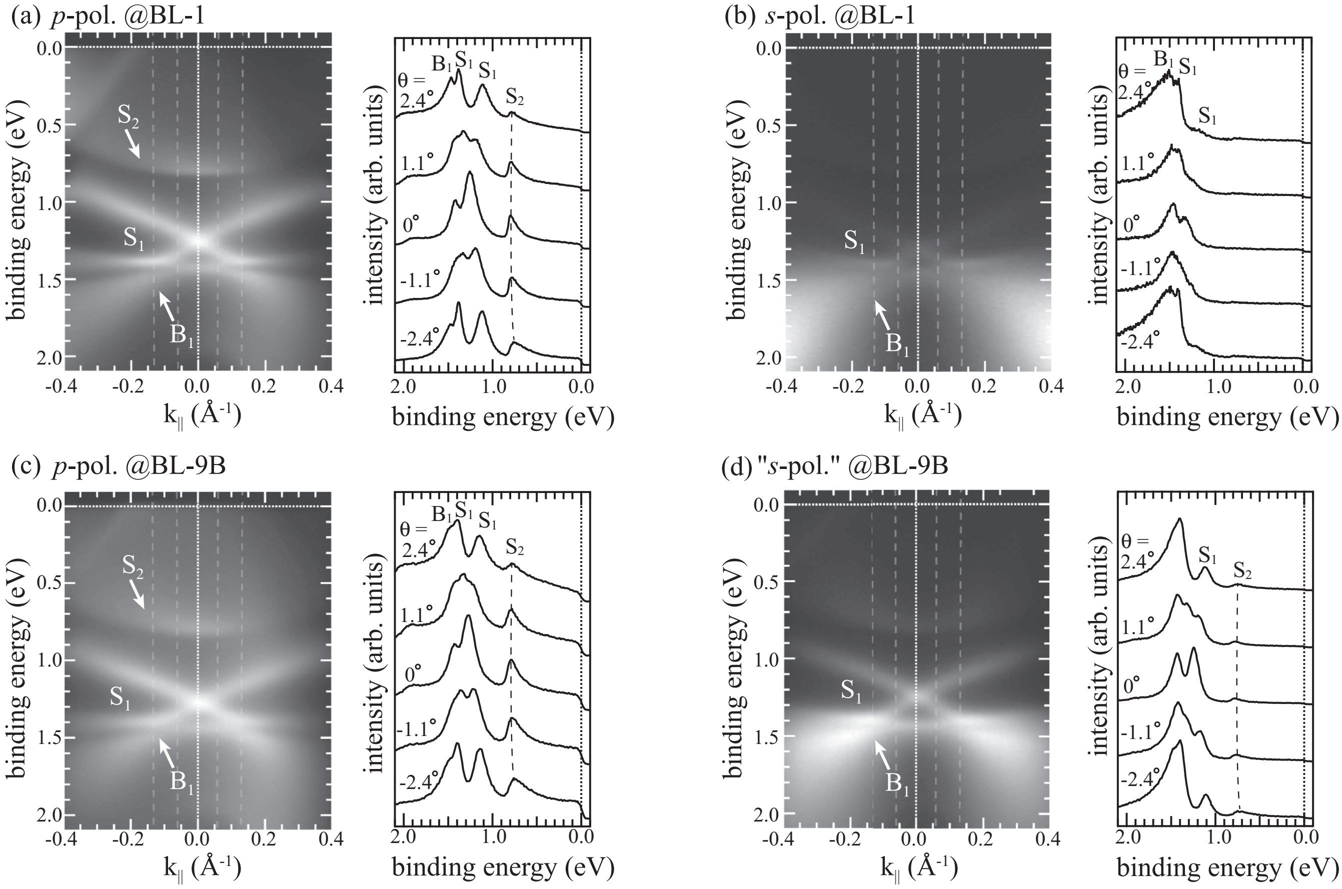

FIG. 1. ARPES results for W(110) along $\overline{\Gamma}\,\overline{\mathrm{H}}$ obtained for *p*- and *s*-polarized light of $h\nu = 43$ eV at BL-1 [(a) and (b)] and BL-9B [(c) and (d)]. The photoemission intensities are presented as contour plots $E(\mathbf{k}_\parallel)$ on a linear gray scale as well as energy distribution curves (EDCs) for selected emission angles $\theta = 0^\circ, \pm 1.1^\circ, \pm 2.4^\circ$, corresponding to $k_\parallel$ values as indicated by dashed lines.

in this study, in which we aim to extract the spin texture of a minor spectral contribution excited exclusively by *s*-polarized light. To clearly identify orbital symmetries of the respective states, we used BL-1 for measurements with complete *p* and *s* polarization yet without spin-polarization detection. The complete linear polarization at BL-1 is preserved on changing the polarization plane by rotating the whole ARPES apparatus with respect to the synchrotron beam.

At both beamlines, the angle of light incidence was 50° relative to the lens axis of the electron analyzer. The overall experimental energy and angle resolutions of ARPES at BL-1 (BL-9B) were set to 15 meV (50 meV) and 0.2° (0.3°). Those of spin-ARPES at BL-9B were 50 meV and 0.75°. The spin-ARPES system can resolve both out-of-plane (P_z) and two in-plane (P_x and P_y) spin-polarization components. In this work, only one spin component (P_y, perpendicular to $\mathbf{k}_\parallel$) was measured, which is the only symmetry-allowed spin polarization direction along $\overline{\Gamma}\,\overline{\mathrm{H}}$ of a bcc(110) surface. The emission angle θ of the photoelectrons is defined as positive (negative), when the surface normal is moved away from (toward) the light propagation vector. All measurements have been performed at a sample temperature of 80 K.

Figures 1(a) and 1(b) show spin-integrated ARPES data for W(110) along $\overline{\Gamma}\,\overline{\mathrm{H}}$ obtained from BL-1 with pure *p*-polarized and *s*-polarized light of $h\nu = 43$ eV. For *p*-polarized light [Fig. 1(a)], we observe three characteristic features, a Dirac-cone-like state S_1, a surface-state emission S_2, and a bulk emission B_1, as identified before [19,20]. S_1 clearly shows an almost-linear energy dispersion with a crossing point at a binding energy E_B of 1.25 eV at $\overline{\Gamma}$. In the case of *s*-polarized light [Fig. 1(b)], the intensity of S_1 is strongly reduced and the intensity of S_2 is completely lost. This demonstrates that S_1 has predominantly and S_2 completely even symmetry.

Equivalent ARPES spectra obtained from BL-9B are presented in Figs. 1(c) and 1(d). The results for *p*-polarized light [Fig. 1(c)] are identical to the results obtained from BL-1 [Fig. 1(a)] except for differences in linewidths that depend on the settings of the energy and angle resolutions in both experiments. For *s*-polarized light, however, the ARPES results from BL-9B [Fig. 1(d)] differ significantly from those from BL-1 [Fig. 1(b)]: The intensity of S_2 is not lost and the Dirac-cone-like dispersion behavior of S_1 is clearly visible. This discrepancy is caused by the admixture of *p*-polarized light in the nominal *s*-polarized light. Even a small contribution of *p*-polarized light leads to significant intensity for S_1 due to the strong photoionization cross section. It is, however, favorable that S_2 is exclusively excited by *p*-polarized light. This information can be used to remove the *p*-induced intensity contribution of S_1 from the nominal *s*-induced intensity in the spin-resolved spectra.

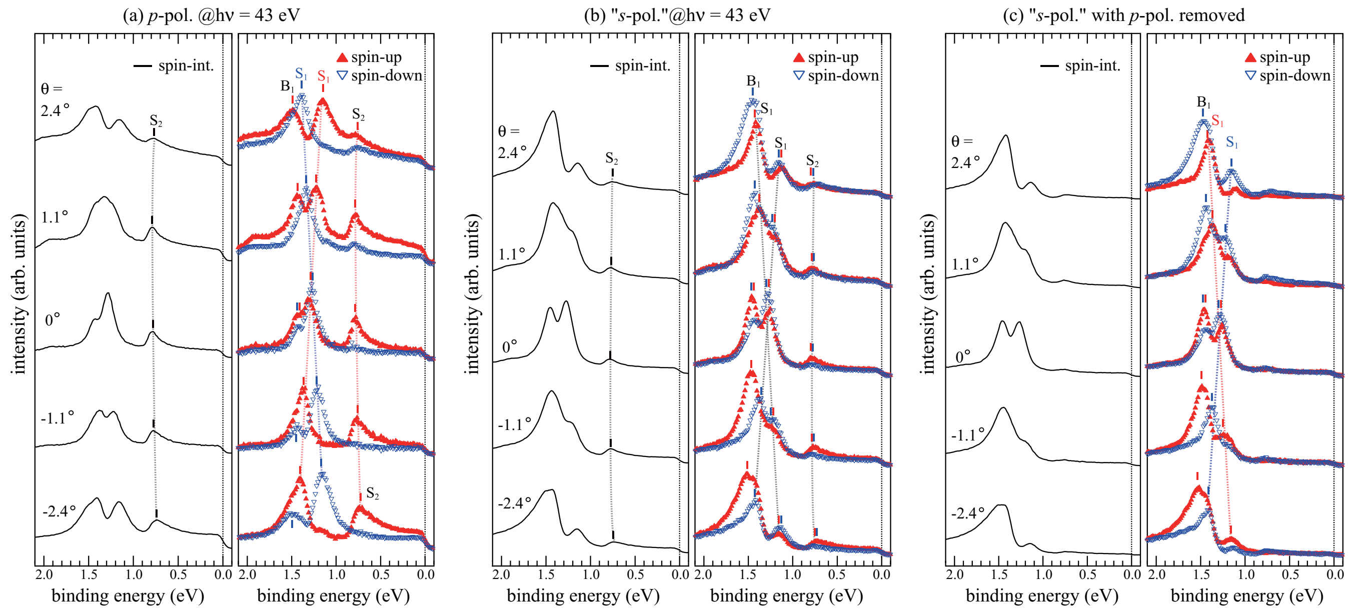

FIG. 2. Spin-integrated and spin-resolved EDCs for W(110) along $\overline{\Gamma}\,\overline{\mathrm{H}}$ obtained with p-polarized (a) and nominal s-polarized light (b) at BL-9B. Panel (c) shows the results where the p contribution has been removed from the spectra obtained with nominal s-polarized light. See text for details.

Figures 2(a) and 2(b) show spin-integrated and spin-resolved ARPES data as energy distribution curves (EDC) excited with p- and s-polarized light from BL-9B. Spin-up (I^{up}) and -down (I^{down}) intensities are plotted with pointing-up and -down triangles, respectively. For normal emission, the results for p-polarized light [Fig. 2(a)] show three features: B_1 at $E_{\mathrm{B}} = 1.45$ eV, S_1 at 1.25 eV in both spin channels, and S_2 as a sharp spin-up peak at 0.78 eV. In the spectra for positive (negative) θ, the spin-up (spin-down) peak B_1 shifts to higher E_{B} with increasing (decreasing) θ. The spin-up peak S_2 shifts slightly to lower E_{B} with increasing $|\theta|$. For the prominent feature S_1, the spin-down peak shifts to higher E_{B} with increasing θ, while the spin-up peak shifts to lower E_{B}. These observations confirm a Dirac-cone-like dispersion behavior and spin texture of S_1, reminiscent of a TSS, as previously shown [19,25]. The bulk-derived feature B_1 shows a Rashba-type spin texture, which reminds us of the behavior of bulk states on Bi(111) [29]. Note that our spectra show not only the **k**-dependent intrinsic spin texture of the respective states. Due to the broken symmetry by the experimental geometry, **k**-independent spin polarization is observed in addition; see, e.g., the dominating spin-up polarization for all angles of electron incidence for excitation with p-polarized light in Fig. 2(a). This effect has been discussed in detail in the literature [12,15,25,30].

The spectra for nominal s-polarized light [Fig. 2(b)] show similar spectral features but with modified intensities. The spin-resolved data, however, differ considerably from the results for p-polarized light. While the spin polarization of B_1 appears almost reversed when changing the sign of θ, the spin polarization of S_1 is almost lost. To understand this behavior, the admixture of p polarization in the s-polarized light has to be taken into account, which manifests itself in the nonvanishing intensity of S_2. To eliminate this experimental artifact, we subtracted spin-resolved spectra excited by p-polarized light from spectra excited by nominal s-polarized light. The weighting coefficient R used for subtraction was derived from the intensity of the spin-integrated peak S_2, which is exclusively excited by p-polarized light:

$$I^i_{s-\mathrm{pol}} = I^i_{\text{“}s-\mathrm{pol}\text{”}} - R I^i_{p-\mathrm{pol}}. \qquad (1)$$

Here, $I^i_{s-\mathrm{pol}}$ ($I^i_{p-\mathrm{pol}}$) and $I^i_{\text{“}s-\mathrm{pol}\text{”}}$ denote spectral intensities excited by completely s-polarized (p-polarized) light and nominal s-polarized light, respectively. The upper index i denotes spin-up and spin-down. R is the ratio between photoemission intensities of S_2 for excitation with “s”- and p-polarized light. An estimate for R (0.08 to 0.12) is derived from the polarization-dependent results for S_2. The uncertainty in R is caused by a changing light intensity as well as aging effects of the sample condition, which lead to slightly changing intensities in the spectra used for the subtraction procedure. This also explains why S_2 could not be completely eliminated in Fig. 2(c). With this approach, we were able to reconstruct spin-resolved spectra for fully s-polarized light in a semiquantitative way [Fig. 2(c)]. More importantly, we are now able to reveal the true spin texture of S_1, when excited with s-polarized light: It is reversed in comparison with the p-polarized case.

This switching spin feature of S_1 is reproduced by our first-principles calculations including the photoemission process in the one-step model as described in Ref. [22]. Figure 3 shows spin-integrated ARPES intensities $I^{\mathrm{up}} + I^{\mathrm{down}}$ [Figs. 3(a) and 3(d)], intensity differences $I^{\mathrm{up}} - I^{\mathrm{down}}$ [Figs. 3(b) and 3(e)] and spin-resolved EDCs [Figs. 3(c) and 3(f)] calculated for W(110) along $\overline{\Gamma}\,\overline{\mathrm{H}}$ for excitation with 100% p- [Figs. 3(a)–3(c)] and 100% s-polarized light [Figs. 3(d) and 3(f)] of $h\nu = 43$ eV. S_2 appears only for excitation with p-polarized light and the spin polarization of the bulk continuum state B_1 is reversed on switching the linear

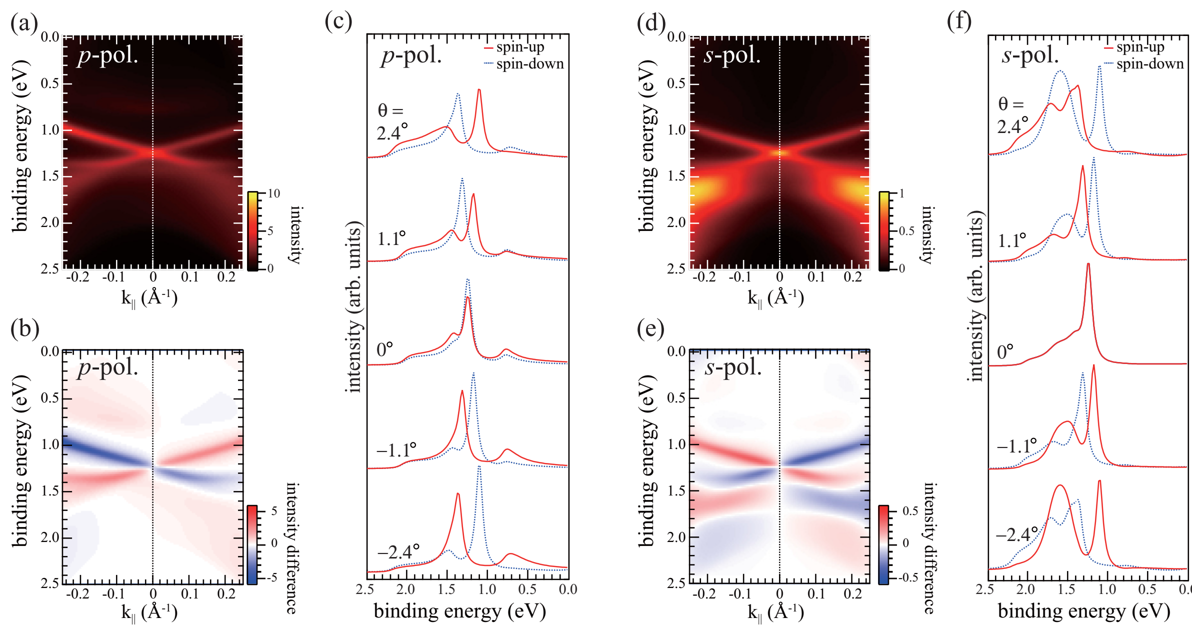

FIG. 3. Spin-integrated and spin-resolved ARPES intensities calculated for W(110) along $\overline{\Gamma}\,\overline{\text{H}}$ within the one-step model of photoemission. Note that the intensities for p-polarized light are about 10 times higher than for s-polarized light. Panels (a)–(c) [(d)–(f)] show the calculated spectra excited by the photon energy of 43 eV with p- (s-)polarized light. [(b) and (e)] Intensity differences between spin-up and spin-down excited by p- and s-polarized light, respectively. [(c) and (f)] spin-resolved EDC spectra with several emission angles.

polarization of the exciting light, all in agreement with our experimental observations.

The calculations provide detailed information about S_1. According to dipole section rules for photoelectrons in our experimental geometry, even and odd orbital symmetry in the initial state can be excited by p- and s-polarized light, respectively. Considering group theory including spin-orbit interaction under mirror symmetry, the wave function of a spin-orbit-induced spin-split band consists of $a_1|\text{even},\uparrow\rangle + a_2|\text{odd},\downarrow\rangle$ or $a_1|\text{even},\downarrow\rangle + a_2|\text{odd},\uparrow\rangle$ ($|a_1|^2 \neq |a_2|^2$). Here $\uparrow$ and $\downarrow$ correspond to spin alignment with direction perpendicular to the mirror plane (P_y in the experimental geometry). The calculated intensities for s-polarized light are about 1/10 of those for p-polarized light [Figs. 3(a) and 3(d)]. According to the electronic structure calculation, the Dirac-cone-like surface state for W(110) is composed of even symmetry (Σ_1 and Σ_3) with more than 90% spectral weight and odd symmetry (almost only Σ_2) with less than 10% spectral weight with opposite spin polarization. The photoionization cross section of S_1 for p-polarized light is, therefore, about 10 times higher than that for s-polarized light. As a consequence, a small p admixture in the experimental s-polarized light has significant influence on the results for S_1. In the case of 10% p admixture, no spin polarization is expected for S_1 in the experimental data for nominal s-polarized light. This is exactly what we observe: Figure 3(b) shows almost equal intensities of S_1 for spin-up and spin-down. This result provides an estimate for the ratio of the coefficients a_1/a_2 of about 9 in the initial state. Consequently, the spin polarization of the Dirac-cone-like surface state S_1 is roughly 80%.

In summary, we have revealed the orbital-symmetry-selective spin texture of the d-derived Dirac-cone-like surface state on W(110) with C_{2v} crystal symmetry using spin-resolved ARPES measurements excited by p- and s-polarized light. Along the mirror-plane high-symmetry direction $\overline{\Gamma}\,\overline{\text{H}}$, a predominant part of the state has even symmetry and shows a spin texture, which is opposite in sign to the spin structure of a minor part with odd symmetry. This result unveils in which way spin-orbit interaction combines spin and orbital degrees of freedom. Compared with recent results for the topological surface state in Bi_2Se_3, which consists of p-type orbitals at a surface with C_{3v} symmetry, we conclude that “spin control” is not restricted to topological insulators but a much more general phenomenon.

The measurements were performed with the approval of the Proposal Assessing Committee of HSRC (Proposal Nos. 10-A-27, 13-B-2). We thank S. Sasaki for stimulating discussions. H.W. and M.D. gratefully acknowledge the hospitality of HiSOR. This work was financially supported by KAKENHI (Grants No. 23340105, No. 23244066, and No. 25800179), Grants-in-Aid for Scientic Research (A) and (B) and for Young Scientists (B) of JSPS.

[1] Y. A. Bychkov and E. I. Rashba, Properties of a 2D electron gas with lifted spectral degeneracy, JETP Lett. **39**, 78 (1984).

[2] S. Datta and B. Das, Electronic analog of the electro-optic modulator, Appl. Phys. Lett. **56**, 665 (1990).

[3] I. M. Miron, G. Gaudin, S. Auffret, B. Rodmacq, A. Schuhl, S. Pizzini, J. Vogel, and P. Gambardella, Current-driven spin torque induced by the Rashba effect in a ferromagnetic metal layer, Nat. Mater. **9**, 230 (2010).

[4] M. Z. Hasan and C. L. Kane, Topological insulators, Rev. Mod. Phys. **82**, 3045 (2010).

[5] C. Jozwiak, C.-H. Park, K. Gotlieb, C. Hwang, D.-H. Lee, S. G. Louie, J. D. Denlinger, C. R. Rotundu, R. J. Birgeneau, Z. Hussain, and A. Lanzara, Photoelectron spin-flipping and texture manipulation in a topological insulator, Nat. Phys. **9**, 293 (2013).

[6] Z.-H. Zhu, C. N. Veenstra, G. Levy, A. Ubaldini, P. Syers, N. P. Butch, J. Paglione, M. W. Haverkort, I. S. Elfimov, and A. Damascelli, Layer-by-Layer Entangled Spin-Orbital Texture of the Topological Surface State in Bi_2Se_3, Phys. Rev. Lett. **110**, 216401 (2013).

[7] Yue Cao, J. A. Waugh, X-W. Zhang, J.-W. Luo, Q. Wang, T. J. Reber, S. K. Mo, Z. Xu, A. Yang, J. Schneeloch, G. D. Gu, M. Brahlek, N. Bansal, S. Oh, A. Zunger, and D. S. Dessau, Mapping the orbital wavefunction of the surface states in three-dimensional topological insulators, Nat. Phys. **9**, 499 (2013).

[8] H. Zhang, C.-X. Liu, and S.-C. Zhang, Spin-Orbital Texture in Topological Insulators, Phys. Rev. Lett. **111**, 066801 (2013).

[9] Z.-H. Zhu, C. N. Veenstra, S. Zhdanovich, M. P. Schneider, T. Okuda, K. Miyamoto, S.-Y. Zhu, H. Namatame, M. Taniguchi, M. W. Haverkort, I. S. Elfimov, and A. Damascelli, Photoelectron Spin-Polarization Control in the Topological Insulator Bi_2Se_3, Phys. Rev. Lett. **112**, 076802 (2014).

[10] Zhuojin Xie, Shaolong He, Chaoyu Chen, Ya Feng, Hemian Yi, Aiji Liang, Lin Zhao, Daixiang Mou, Junfeng He, Yingying Peng, Xu Liu, Guodong Liu, Xiaoli Dong, Li Yu, Jun Zhang, Shenjin Zhang, Zhimin Wang, Fengfeng Zhang, Feng Yang, Qinjun Peng, Xiaoyang Wang, Chuangtian Chen, Zuyan Xu, and X. J. Zhou, Orbital-selective spin texture and its manipulation in a topological insulator, Nat. Commun. **5**, 3382 (2014).

[11] J. Sánchez-Barriga, A. Varykhalov, J. Braun, S.-Y. Xu, N. Alidoust, O. Kornilov, J. Minár, K. Hummer, G. Springholz, G. Bauer, R. Schumann, L. V. Yashina, H. Ebert, M. Z. Hasan, and O. Rader, Photoemission of Bi_2Se_3 with Circularly Polarized Light: Probe of Spin Polarization or Means for Spin Manipulation?, Phys. Rev. X **4**, 011046 (2014).

[12] U. Heinzmann and J. H. Dil, Spin orbit induced photoelectron spin polarization in angle resolved photoemission from both atomic and condensed matter targets, J. Phys.: Condens. Matter **24**, 173001 (2012).

[13] J. Osterwalder, Can spin-polarized photoemission measure spin properties in condensed matter?, J. Phys.: Condens. Matter **24**, 171001 (2012).

[14] S. N. P. Wissing, A. B. Schmidt, H. Mirhosseini, J. Henk, S. R. Ast, and M. Donath, Ambiguity of Experimental Spin Information from States with Mixed Orbital Symmetries, Phys. Rev. Lett. **113**, 116402 (2014).

[15] H. Wortelen, H. Mirhosseini, K. Miyamoto, A. B. Schmidt, J. Henk, and M. Donath, Tuning the spin signal from a highly symmetric unpolarized electronic state, Phys. Rev. B **91**, 115420 (2015).

[16] L. Bawden, J. M. Riley, C. H. Kim, R. Sankar, E. J. Monkman, D. E. Shai, H. I. Wei, E. B. Lochocki, J. W. Wells, W. Meevasana, T. K. Kim, M. Hoesch, Y. Shtsubo, P. Le Fèvre, C. J. Fennie, K. M. Shen, F. Chou, and P. D. C. King, Hierarchical spin-orbital polarization of a giant Rahsba system, Sci. Adv. **1**, e1500495 (2015).

[17] R. H. Gaylord and S. D. Kevan, Spin-orbit-interaction-induced surface resonance on W(011), Phys. Rev. B **36**, 9337 (1987).

[18] J. Feydt, A. Elbe, H. Engelhard, G. Meister, Ch. Jung, and A. Goldmann, Photoemission from bulk bands along the surface normal of W(110), Phys. Rev. B **58**, 14007 (1998).

[19] K. Miyamoto, A. Kimura, K. Kuroda, T. Okuda, K. Shimada, H. Namatame, M. Taniguchi, and M. Donath, Spin-Polarized Dirac-Cone-Like Surface State with d Character at W(110), Phys. Rev. Lett. **108**, 066808 (2012).

[20] K. Miyamoto, A. Kimura, K. Kuroda, T. Okuda, K. Shimada, H. Iwasawa, H. Hayashi, H. Namatame, M. Taniguchi, and M. Donath, Massless or heavy due to two-fold symmetry: Surface-state electrons at W(110), Phys. Rev. B **86**, 161411(R) (2012).

[21] A. G. Rybkin, E. E. Krasovskii, D. Marchenko, E. V. Chulkov, A. Varykhalov, O. Rader, and A. M. Shikin, Topology of spin polarization of the 5*d* states on W(110) and Al/W(110) surfaces, Phys. Rev. B **86**, 035117 (2012).

[22] H. Mirhosseini, M. Flieger, and J. Henk, Dirac-cone-like surface state in W(110): Dispersion, spin texture and photoemission from first principles, New J. Phys. **15**, 033019 (2013).

[23] H. Mirhosseini, F. Giebels, H. Gollisch, J. Henk and R. Feder, *Ab initio* spin-resolved photoemission and electron pair emission from a Dirac-type surface state in W(110), New J. Phys. **15**, 095017 (2013).

[24] J. Braun, K. Miyamoto, A. Kimura, T. Okuda, M. Donath, H. Ebert, and J. Minár, Exceptional behavior of d-like surface resonances on W(110): the one-step model in its density matrix formulation, New. J. Phys. **16**, 015005 (2014).

[25] K. Miyamoto, A. Kimura, T. Okuda, and M. Donath, Spin polarization of surface states on W (110): Combined influence of spin-orbit interaction and hybridization, J. Electron. Spectrosc. Relat. Phenom. **201**, 53 (2015).

[26] S. Sasaki, A. Miyamoto, K. Goto, M. Arita, T. Okuda, T. Mitsuyasu, K. Fujioka, H. Namatame, and M. Taniguchi, Quasi-periodic variably polarizing undulator at HiSOR, J. Phys. Conf. Ser. **425**, 032009 (2013).

[27] T. Okuda, K. Miyamoto, H. Miyahara, K. Kuroda, A. Kimura, H. Namatame, and M. Taniguchi, Efficient spin resolved spectroscopy observation machine at Hiroshima Synchrotron Radiation Center., Rev. Sci. Instrum. **82**, 103302 (2011).

[28] T. Okuda, K. Miyamoto, A. Kimura, H. Namatame, and M. Taniguchi, A double VLEED spin detector for high-resolution three dimensional spin vectorial analysis of anisotropic Rashba spin splitting, J. Electron Spectrosc. Relat. Phenom. **201**, 23 (2015).

[29] A. Kimura, E. E. Krasovskii, R. Nishimura K. Miyamoto, T. Kadono, K. Kanomaru, E. V. Chulkov, G. Bihlmayer, K. Shimada, H. Namatame, and M. Taniguchi, Strong Rashba-Type Spin Polarization of the Photocurrent from Bulk Continuum States: Experiment and Theory for Bi (111), Phys. Rev. Lett. **105**, 076804 (2010).

[30] C. Jozwiak, Y. L. Chen, A. V. Fedorov, J. G. Analytis, C. R. Rotundu, A. K. Schmid, J. D. Denlinger, Y.-D. Chuang, D.-H. Lee, I. R. Fisher, R. J. Birgeneau, Z.-X. Shen, Z. Hussain, and A. Lanzara, Widespread spin polarization effects in photoemission from topological insulators, Phys. Rev. B **84**, 165113 (2011).